Application Of Seismic Interferometry With Non-Physical Reflections Using Near-Surface Seismic Field Data

Shirmohammadi, F.; Draganov, D.S.; Balestrini, F.I.; Ghose, R.

DOI
10.3997/2214-4609.202220075

Publication date
2022

Document Version
Final published version

Published in
28th European Meeting of Environmental and Engineering Geophysics

EAGE

CONFERENCE & EXHIBITION
NEAR SURFACE GEOSCIENCE'22

APPLICATION OF SEISMIC INTERFEROMETRY WITH NON-PHYSICAL REFLECTIONS USING NEAR-SURFACE SEISMIC FIELD DATA

F. Shirmohammadi[1], D. Draganov[1], F. Balestrini[1], R. Ghose[1]

[1] Delft University of Technology

Summary

Seismic interferometry (SI) is a method that retrieves new seismic traces from the cross-correlation of existing traces, where one of the receivers acts as a virtual seismic source whose response is retrieved at other receivers. When using sources only at the surface, and the so-called one-sided illumination of the receivers occurs, we will retrieve not only the desired physical reflections but also non-physical (ghost) reflections. These non-physical reflections appear due to waves that propagate inside a subsurface layer. Thus, they contain information about the seismic properties of the specific layer.
We illustrate the technique's potential using numerically modelled data for a subsurface model with a low-velocity layer, which is also pinching out, and near-surface field data. We apply SI by cross-correlation and auto-correlation. Both resulting non-physical reflections are sensitive to the physical rock properties of the layer that causes them to appear in the SI results. Moreover, non-physical reflections in zero-offset gathers that result from SI by auto-correlation show very good conformity with the geometry of the subsurface layers.

Application of seismic interferometry with non-physical reflections using near-surface seismic field data

Introduction

Seismic interferometry (SI) refers to generating seismic responses by cross-correlating seismic observations at different receiver locations (Wapenaar and Fokkema, 2006). The theory assumes certain conditions including that the boundary sources emit the same energy, have regular spacing, and are spaced densely enough. When the assumptions are not met in body-wave SI, not only the desired physical reflections will be retrieved, but also non-physical (ghost) reflections (Snieder et al., 2006; Draganov et al., 2013). The non-physical reflections are caused by internal reflections inside subsurface layers or by extra propagation of primaries between two depth levels, and they are particularly important for monitoring changes in the specific subsurface layer that causes them to appear in the SI result because they could provide valuable information about the physical rock properties of the subsurface.

This approach has been applied to different scales using laboratory data and numerical modelling but not with field dataset. King et al. (2011) showed that ghost reflections could be used in velocity-analysis processing to estimate subsurface velocities better. Draganov et al. (2012) proposed the use ghost reflections for monitoring CO_2. By using realistic numerical modelling from a horizontally layered model, they showed that apart from physical reflection, the non-physical reflections are retrieved, which are sensitive to the thickness and velocity of the layers. They also simulated the replacement of CO_2 in a laboratory test, and showed a trend of velocity changes similar to the observed one with direct transmission measurements. Similarly, Draganov et al. (2013) applied SI to records from receivers at the Earth`s surface from sources in wells. They showed that by using a vertical well, ghost reflections could be identified; using receivers inside a horizontal well, the identified ghost reflections can then be employed to monitor the velocity and Q factor changes inside layers.

We illustrate the potential of ghost reflections with data from numerical acoustic modelling for a subsurface model with a low-velocity layer that is also pinching out. With multi-offset gathers, both physical and ghost reflections are retrieved; by muting undesired reflections in the data before application of SI, we can better retrieve target ghost reflections. With zero-offset gathers retrieved from SI by auto-correlation (AC), the ghost reflections show a very good agreement with the geometry of specific subsurface layers. We also investigate the utilization of ghost reflections retrieved using a near-surface field dataset collected near Rotterdam in the Netherlands. We retrieve zero-offset gathers by turning shots into the virtual receivers and receivers into virtual sources. In both cases, a similar trend for the ghost reflection is observed, imaging directly the target specific layer.

Method

The acoustic Green's function $G(\boldsymbol{x}_B, \boldsymbol{x}_A, t)$ and its time-reversed variant at a receiver at $\boldsymbol{x}_B$ from a virtual source at $\boldsymbol{x}_A$ can be obtained from observations at the receivers at $\boldsymbol{x}_A$ and $\boldsymbol{x}_B$ at the surface using the relation (Wapenaar and Fokkema, 2006)

$$G(\boldsymbol{x}_A, \boldsymbol{x}_B, t) + G(\boldsymbol{x}_A, \boldsymbol{x}_B, -t) \approx \frac{2}{\rho c} \oint_{\partial \mathrm{D}} G(\boldsymbol{x}_B, \boldsymbol{x}, t) * G(\boldsymbol{x}_A, \boldsymbol{x}, -t)\, d^2x, \quad (1)$$

where c and ρ are the constant propagation velocity and mass density, respectively, at and outside the source-boundary surface ∂D, which effectively surrounds $\boldsymbol{x}_A$ and $\boldsymbol{x}_B$; $*$ denotes convolution. The right-hand side of relation 1 is the cross-correlation (CC) of recordings at the points $\boldsymbol{x}_A$ and $\boldsymbol{x}_B$ from sources at positions $\boldsymbol{x}$ on ∂D in the subsurface. When the positions $\boldsymbol{x}$ are at the surface, as in a typical active-source exploration survey, the requirement about ∂D to effectively surround the receivers is not met, leading to non-physical arrivals (ghosts) being retrieved in the Green's function estimates.

In relation 1, if we substitute $\boldsymbol{x}_A$ instead of $\boldsymbol{x}_B$, the retrieved Green's function is the result of auto-correlation of the arrivals at the receiver $\boldsymbol{x}_A$, which means $\boldsymbol{x}_A$ acts as a virtual source and receiver. The retrieved traces would thus represent a zero-offset reflection section. We apply relation 1 by CC and auto-correlation (AC) to simulated reflection experiments and to near-surface field data.

Examples

For the explanation of the method, we use a subsurface model with a low-velocity layer (Figure 1), which is also pinching out, with receivers (blue triangles in Figure 1) at the free surface between 3000–5000 m placed every 20 m and sources (red stars in Figure 1) at the surface evenly distributed in the horizontal direction every 40 m between 1010-5010 m. To better compare the SI result with the directly modelled one, we show the directly modelled result for a source at 3000 m in Figure 2a. We use a finite-difference modelling code (Thorbecke and Draganov, 2011) in an acoustic mode to generate a seismic reflection dataset.

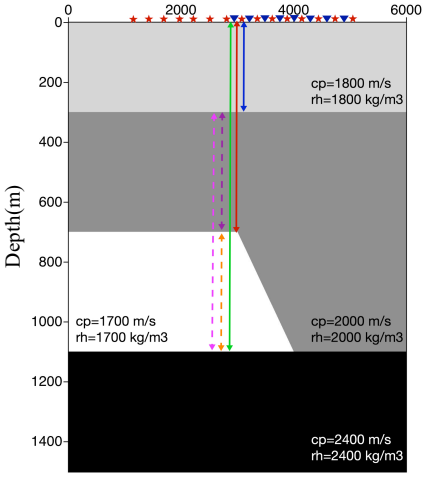

Figure 1. *Subsurface model. The stars represent sources, the triangles –receivers, and the coloured rays illustrate several reflection paths. Blue: a reflection from the bottom of the first layer, Red: a reflection from the bottom of the second layer, Green: a reflection from the bottom of the third layer; Violet: correlation result of the blue and red rays – reflection inside the second layer; Orange: correlation result of the red and green rays – reflection inside the third layer; and Magenta: correlation result of the blue and green rays – reflection inside the second and the third layer.*

We perform SI by AC and by CC. Figure 2(b) shows the retrieved results of SI by CC. We retrieve not only the physical reflections but also ghost reflections, which are the results of the correlation process that cancel the common ray paths. We can utilize all panels as input, but to better retrieve ghost reflections, one idea is muting the arrivals recorded before and after the desired reflections. Figure 2(c) shows the retrieved result of SI by CC for a virtual source at 3000 m when we use reflection panels with muted arrivals before the reflection from the bottom of the 1st layer (as the arrival indicated by the blue arrow in Figure 2a) and after the reflection from the bottom of the 3rd layer (as the arrival indicated by the green arrow in Figure 2a).

By comparing the retrieved results of SI (Figures 2b-c) with the directly modelled reflection response (Figure 2a), we can see that apart from the physical arrivals (the blue, red, and green arrivals), there are also ghost reflections (the magenta, violet, and orange arrival). These ghost reflections represent reflection arrivals from inside separate subsurface layers (see the corresponding colours in Figure 1) as if measured with sources and receivers placed directly at the top of each layer. Comparing the result in Figure 2c to the result in Figure 2b, we can see that the retrieved ghost reflections are clearer and stronger by selecting and correlating specific arrivals in the recorded reflection panels (Figure 2a). Using SI by AC, the zero-offset ghost reflections can be retrieved at each of the receiver locations (Figure 2d). The zero-offset ghost reflections show a very good conformity with the geometry of the specific subsurface interfaces, see e.g., the violet arrival.

We apply our knowledge about retrieving ghost reflections to field data to test how our procedure works. The site where the data was recorded is located in the western part of the Netherlands, near Rotterdam. The total profile length was 190 m with a shot and receiver interval of 1.0 m and 0.5 m, respectively.

The geology of this site, known from earlier borehole measurements, comprises flat alternating layers of Holocene clay and sand (Figure 3a-b). The sand is relatively homogeneous. In the topmost part (Holocene), the appearance of sand layers at around 1–2 m, 4–5 m, and 7–12 m depths were marked in several boreholes (Ghose and Goudswaard, 2004).

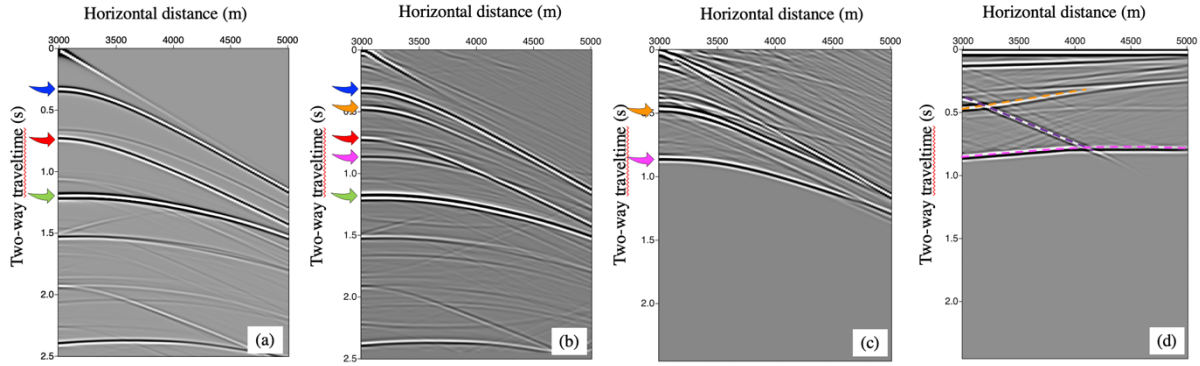

Figure 2. (a) *Directly modelled reflection response for an actual source at (3000,0) m. The blue, red, and green arrows indicate the reflections from the bottom from the 1st, 2nd, and 3rd layer, respectively.* ***(b)*** *Result of SI by CC applied to panels as in (a) for a virtual source at (3000,0) m.* ***(c)*** *Result of SI by CC for a virtual source at (3000,0) m applied to panels with muted arrivals before the reflections from the bottom of the 1st layer and after the reflection from the bottom of the 3rd layer.* ***(d)*** *Results of SI by autocorrelation of muted panels containing only reflections from the bottom of the 1st layer and the bottom of the 2nd and 3rd layer. The orange, violet, and magenta arrows and dashed lines indicate the retrieved ghost reflections corresponding to the colours in Figure 1.*

Using tapered muting, we extract two of the earliest reflections on the shot gathers (indicated by the transparent blue area in Figure 3c) after eliminating surface waves and free-surface multiples. Then, we apply SI by AC to them. We apply SI by turning sources into virtual receivers (Figure 4a) but also by turning the receivers into virtual sources (Figure 4b). When we turn the sources into virtual receivers, the traces with the spacing of 0.5 m are stacked, corresponding to the receivers' spacing. So, they are more reliable because the spacing of the stacked traces is shorter than the minimum dominant wavelength. When we turn the receivers into virtual sources, the spacing of the staked traces is similar to the minimum wavelength, but there are more traces in the zero-offset gather. Comparing the result in Figure 4a to the result in Figure 4b, we ascertain the validity of the latter. Thus, for the interspersion, we use both of them.

The SI zero-offset results in Figure 4 exhibit the ghost reflection at 20 ms, related to the specific subsurface layer at a depth of 4-6 m. It shows a generally horizontal event with some changes at 1560-1660 m. Since, based on known geology, we expect to have a horizontal homogeneous layer, this change can be related to the thickness change inside this specific layer, and thus inferences the appearance of the sand layer at this depth.

Conclusions

We used non-physical (ghost) arrivals retrieved from applying seismic interferometry (SI) by cross-correlation (CC) and auto-correlation (AC) to synthetic surface seismic reflection data from a subsurface model with a low-velocity layer, which is also pinching out. We showed that besides the physical reflections also non-physical reflections are retrieved, which propagate inside specific layers. We also showed that the non-physical reflections in zero-offset gathers, retrieved using SI by AC, show a very good agreement with the geometry of the specific subsurface layers, thus allowing imaging, e.g., of pinch-outs. We also retrieved non-physical reflections using SI by AC applied to field data from near-surface measurements. The retrieved zero-offset section exhibits directly the geometry of a sand

layer at a depth of 4-6 m. Using the ghost reflection, we interpreted a change in the thickness of the sand layer.

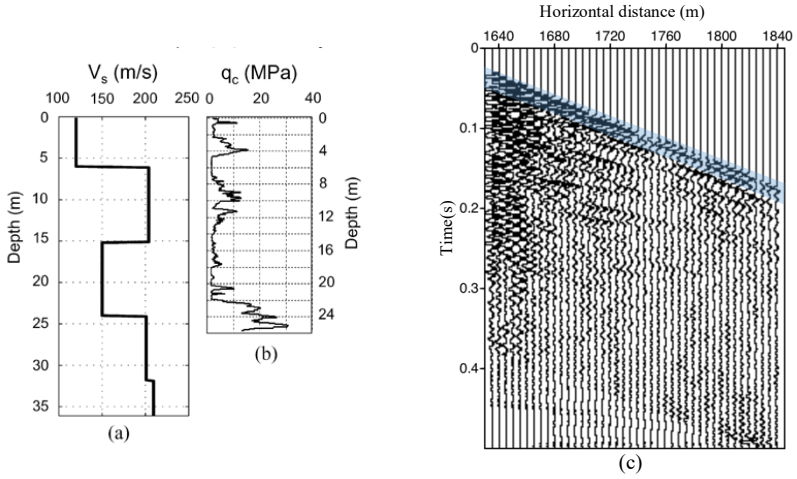

Figure 3. ***(a)*** *Interval velocity obtained from the root-mean-square velocity and* ***(b)*** *cone penetration test cone resistance q_c (Ghose and Goudswaard, 2004).* ***(c)*** *An example shot gather for a source at 1635 m (the blue highlighted region shows the extracted reflection arrivals used for SI by AC)*

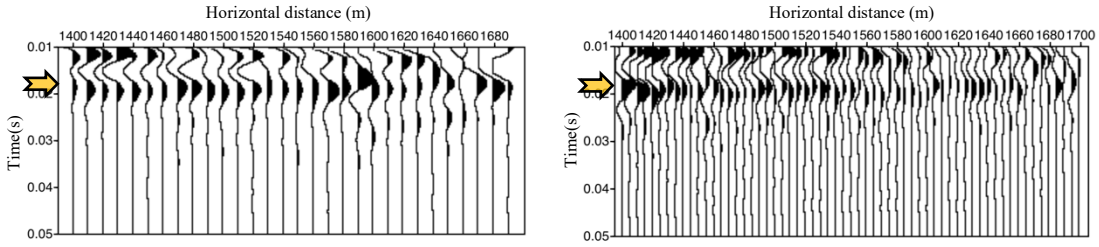

Figure 4. ***(a)*** *Result of SI by AC by turning sources into virtual receivers.* ***(b)*** *Same as (a) but for turning receivers into virtual sources. The orange arrow indicates the retrieved ghost reflection.*

Acknowledgements

This research was (partially) funded by NWO Science domain (NWO-ENW), project DEEP.NL.2018.048

References

Draganov, D., Ghose, R., Heller, K., Ruigrok, E. [2013] Monitoring changes in velocity and Q in reservoirs using non-physical arrivals in seismic interferometry. *Geophys. J. Int.,* **192**., 699-708

Draganov, D., Heller, K., Ghose, R. [2012] Monitoring CO_2 storage using ghost reflections retrieved from seismic interferometry. *Intern. J. Greenh. Gas Control* 11S, S35–S46.

Ghose, R. and Goudswaard, J. [2004] Integrating S-wave seismic-reflection data and cone-penetration-test. *Geophysics*, **69(2)**, 440-459

King, S., Curtis, A., Poole, T.L. [2011] Interferometric velocity analysis using physical and nonphysical energy. *Geophysics*, **76**, SA35–SA49.

Snieder, R., Wapenaar, K., Larner, K. [2006] Spurious multiples in seismic interferometry of primaries. *Geophysics*, **71**, SI111–SI124.

Thorbecke, J., Draganov, D. [2011] Finite-difference modeling for seismic interferometry. *Geophysics*, **76**, H1–H18.

Wapenaar, K. and Fokkema, J. [2006] Green's function representations for seismic interferometry. *Geophysics*, **71(4)**, SI33–SI46.